

# TRANSIENT CFD ANALYSIS OF THE FLOW INVERSION OF THE NUCLEAR RESEARCH REACTOR IEA-R1

N.L. Scuro; P.G. Santos; P.E. Umbehaum; D.A. Andrade;  
*Instituto de Pesquisas Energéticas e Nucleares (IPEN), Centro de Engenharia Nuclear  
Avenida Lineu Prestes, 2242, São Paulo, SP – Brasil*

E. Angelo  
*Universidade Presbiteriana Mackenzie  
Rua da Consolação, 930, São Paulo, SP – Brasil*

G. Angelo  
*Fundação Educacional Inaciana Padre Sabóia de Medeiros (FEI)  
Avenida Humberto de Alencar Castelo Branco, 3972-B, São Bernardo do Campo, SP - Brasil*

## ABSTRACT

The IEA-R1 research reactor works with a downflow direction, but after pumps shutdown during a LOFA test, the reactor shutdown. The heat decay will be removed by natural convection, which is an upward flow, originating flow inversion. Using the Instrumented Fuel Element designed at the Institute for Energy and Nuclear Research (IPEN), the loss of flow accident (LOFA) was analyzed along instrumented fuel plates. The preliminary results showed temperature peaks during inversion, which is as much representative as in nominal operation at 3.5MW. Therefore, these experimental data lead a construction and validation of a transient three-dimensional numerical analysis for a single fuel channel using the ANSYS-CFX® commercial code. The numerical results show improvement in obtaining more properties, e.g., wall heat transfer coefficient, which is usually obtained through empirical correlations.

## 1. Introduction

Numerical modeling is a widely used tool in research reactors, the use of one or bi-dimensional codes have already been tested and validated, thus demonstrating their ability to determine thermo-hydraulic parameters for safety analysis projects with reduced computational time.

These programs aim the calculation of several type of accidents, e.g., loss of flow (LOFA), loss of coolant (LOCA) and even reactive insertion accidents (RIA); however, they face some difficulties at transient state, thus requiring programs that are more robust.

The safety criteria in nuclear tests must be extremely stringent for both energy and research reactors; the use of specific accident codes has been a major requirement to achieve high levels of reliability [1] [2]. As a result, some codes have already been tested and validated for more specific accident conditions, e.g., ATHLET [3], RELAP5 [4]–[6] [7], CATHARE, MERSAT and PARCS, [3] [8].

All of these codes are exemplified in this introduction as part of the state-of-the-art presented in [9], which presents a comparison of the codes: RELAP-5 MOD3.2, PARET-ANL, MTRCR, RELAP-5 MOD3.3, CATHARE, RELAP and MERSAT. These were used for numerical modeling of a LOFA at nuclear research reactor IEA-R1 [10]. To validate the numerical simulations, the experimental procedure was performed using the instrumented fuel element of IPEN (Nuclear and Energy Research Institute - Brazil). Among the results, a satisfactory qualitative and quantitative equivalence was observed for the temperature peaks.

Therefore, the present work represents the initial phase of a transient numerical simulation of the same accident studied by [9], but this time, using a three-dimensional code ANSYS-CFX® [11], which uses the finite volume method. This code considers summarily three-dimensional effects (turbulence) without the use of empirical correlations for the properties calculation.

## 2. Methodology:

This study aims to perform a numerical analysis at transient regime of a LOFA using the methodology of [9]. Information about the experimental procedure are presented below, however, details can be found in the same cited study.

### 2.1 Experimental procedure for the LOFA:

To begin the experimental analysis, the instrumented fuel assembly (IFA) is positioned in the pool for a radial power factor of 0.89 and the whole set of fuel elements is heated up to 3.5MW at steady state. The location of the thermocouple instrumentation is illustrated in Figure 1.

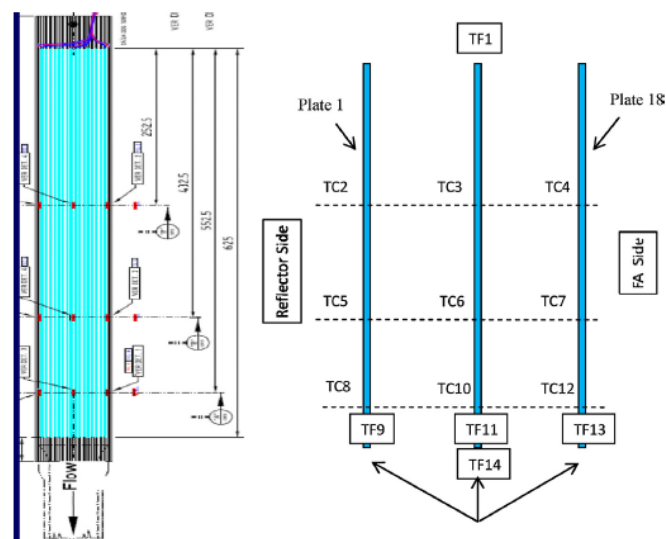


Fig 1. Thermocouples positions - Instrumented Fuel Assembly (IFA)

The nominal flow direction of the IEA-R1 reactor is descending and the connection between all reactor fuel assemblies and the centrifugal pump is made through a set of components. In simplified form, the fuel elements are connected to the matrix plate, which is connected to a hopper. The hopper is connected with a coupling valve, which is purely coupled and decoupled by the pressure difference between the core and the centrifugal pump.

The test starts from the reactor at 3.5MW (steady state) and the accident initiate with the centrifugal pump shutdown, thus the flow of this component is gradually reduced due to the inertia flywheel. However, the 46s of the test, the pressure difference between the core and the pump reaches a limit (27% of nominal flow rate), opening the coupling valve.

Thus, the downward velocity is reduced gradually to zero, where the buoyancy forces promote an upward flow (occurring the inversion between 70s and 100s). The reduction of mass flow after opening the decoupling valve is best described at [7]. This whole process is illustrated by three thermo-hydraulic codes in Figure 2.

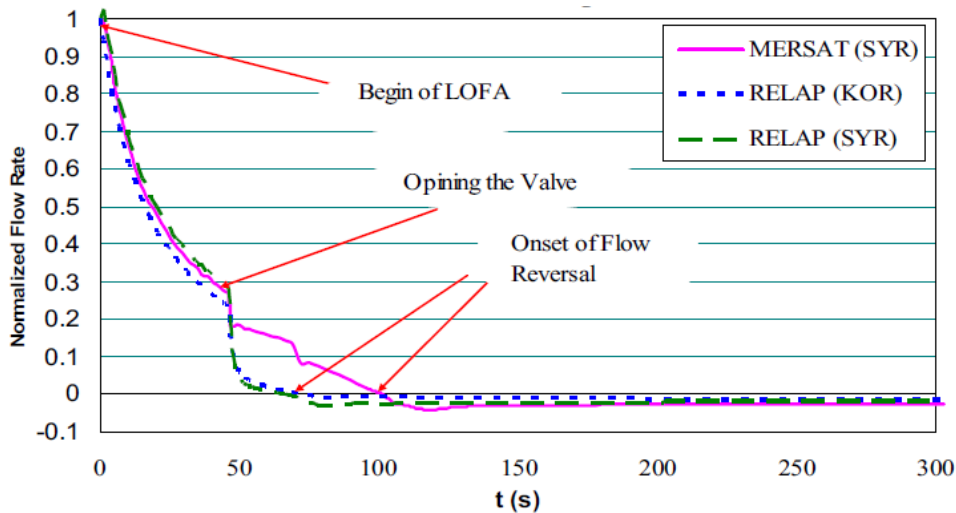


Fig 2. Calculated flow rate evolution during LOFA of IEA-R1

The experimental procedure adjusted to the data acquisition system for a time interval of 1 second, thus, the temperature difference between the thermocouples TF1 (upper thermocouple) and TF11 (lower thermocouple) is illustrated for the entire accident by Figure 3. The same figure also shows all thermo-hydraulic codes answers performed in the study of [9]. It can be observed that the second peak of temperature falls from the moment the natural convection is able to remove more heat than is being generated.

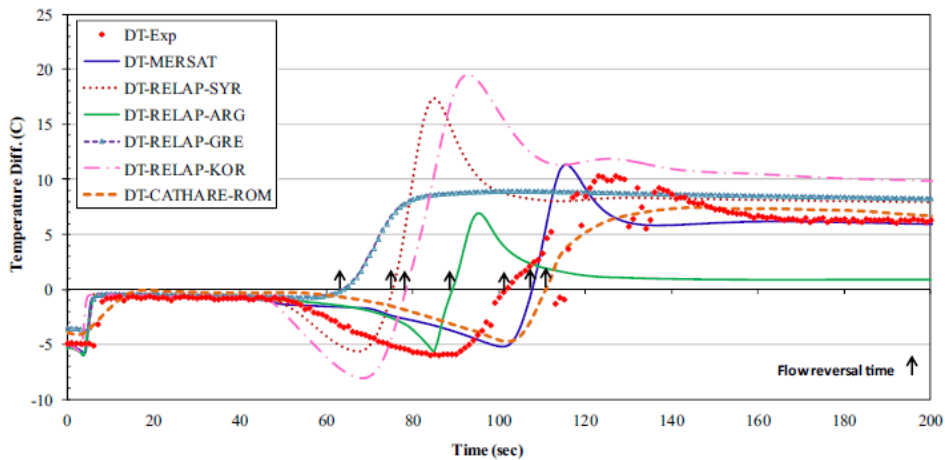


Fig 3. Coolant temperature difference during LOFA of IEA-R1

The experimental uncertainties are described below:

- Deviation in fuel loading per plate: 12%
- Fluctuation in uranium density: 2%
- Error in meat thickness: 10%
- Power measurement: 5%
- Power density variation: 10%
- Flow rate measurement: 3%
- Inlet Pool Temperature 32.7°C – 40°C
- Thermocouple deviation is  $\pm 0.5^\circ\text{C}$  when temperature is minor than 50°C, and  $\pm 0.8^\circ\text{C}$  when greater than 50°C.

### 3. Model Development:

The geometry of the IEA-R1 reactor is described in [10], where the main dimensions required are described below.

- Fuel meat dimensions: 0.76 x 62.6 x 600 [mm]
- Clad thickness: 0.38 [mm]
- Fuel aluminum dimensions: 1.53 x 70.1 x 625 [mm]
- Fluid Channel dimensions: 2.89 x 67.1 x 625 [mm]

It was used 67.1mm in the width of the cladding, instead of 70.1mm, to facilitate the volumetric mesh construction. This simplification does not imply in loss of numerical quality since the difference of 1.5mm for each side of the plate is used to fit on the side plates, where the flow does not occur.

### 4. CFD Analysis:

The mathematical model considers sub-cooled water under transient conditions; the conservation equations follow the simplifying hypotheses of (i) Newtonian fluid and (ii) Boussinesq assumption for the Reynolds stresses. Thus, the equations for mass, momentum and energy are described in Eq. (1), (2) and (3).

$$\frac{\partial \rho}{\partial t} + \frac{\partial}{\partial x_j}(\rho U_j) = 0 \quad (1)$$

$$\frac{\partial}{\partial t}(U_j) + \frac{\partial}{\partial x_j}(\rho U_i U_j) = -\frac{\partial p}{\partial x_i} + \frac{\partial}{\partial x_j}(\tau_{i,j} - \rho \overline{u'_i u'_j}) \quad (2)$$

$$\frac{\partial T}{\partial t} + \frac{\partial}{\partial x_i}(U_i h) = \frac{\partial}{\partial x_i} \left( \lambda \frac{\partial T}{\partial x_i} + \frac{\mu_t}{Pr_t} \frac{\partial h}{\partial x_i} \right) \quad (3)$$

All thermodynamic properties for sub-cooled water were evaluated as a function of temperature and pressure. This procedure is accomplished by the usage of a property table based on the International Association for the Properties of Water and Steam (IAPWS-IF97), and the appropriate formulation for the state equations used in this work is fully described at [12].

Reynolds stress tensor was calculated according to the Boussinesq's hypothesis Eq. (4) and the shear stress can be expressed as indicated by Eq. (5). The effective viscosity, turbulent kinetic energy (k) are shown in Eq. (6) e (7).

$$-\rho \overline{u'_i u'_j} = \mu_t \left( \frac{\partial U_i}{\partial x_j} + \frac{\partial U_j}{\partial x_i} \right) - \frac{2}{3} \delta_{i,j} \left( \rho k + \mu_t \frac{\partial U_k}{\partial x_k} \right) \quad (4)$$

$$\tau_{i,j} = \mu \left( \frac{\partial U_i}{\partial x_j} + \frac{\partial U_j}{\partial x_i} \right) - \frac{2}{3} \mu \delta_{i,j} \frac{\partial U_k}{\partial x_k} \quad (5)$$

$$\mu_{eff} = \mu + \mu_t \quad (6)$$

$$k = \frac{1}{2} \overline{u'_i u'_i} \quad (7)$$

#### 4.1 Turbulence Model:

As this study considers the natural convection phenomenon, the effects near the wall are extremely important. Therefore, as described in the ANSYS-CFX® manual, the k-omega model has a great advantage in the formulation for effects near the wall. This turbulence

models assumes that turbulence viscosity is linked to the turbulence kinetic energy and turbulent frequency via Eq. (8):

$$\mu_t = \rho \frac{k}{\omega} \quad (8)$$

This model was previously postulated by Kolmogorov (1942), however, the numerical model was developed by Wilcox [13]. For the transport equations, the turbulent kinetic energy ( $k$ ), and the turbulent frequency ( $\omega$ ) are expressed by equations (9) and (10).

$$\frac{\delta(\rho k)}{\delta x_j} + \rho \frac{\delta k}{\delta x_i} (\rho \bar{U}_i k) = \frac{\delta}{\delta x_j} \left[ \left( \mu + \frac{\mu_t}{\sigma_k} \right) \frac{\delta k}{\delta x_i} \right] + P_k + P_{kb} - \beta' \rho k \omega \quad (9)$$

$$\frac{\delta(\rho \omega)}{\delta x_j} + \rho \frac{\delta}{\delta x_i} (\rho \bar{U}_i \omega) = \frac{\delta k}{\delta x_i} \left[ \left( \mu + \frac{\mu_t}{\sigma_{\omega 1}} \right) \frac{\delta \omega}{\delta x_i} \right] + \frac{\omega}{k} [(\alpha'_{\omega 1} P_k + P_{\omega b}) - \beta'_{\omega 1} \rho k \omega] \quad (10)$$

Whose constants,  $\alpha'_{\omega 1}$ ,  $\beta'_{\omega 1}$ ,  $\sigma_k$ ,  $\sigma_{\omega 1}$  value equal to 0.09, 5/9, 0.075, 2 e 2, respectively.

The shear turbulent production ( $P_k$ ) due to viscous forces are indicated by Eq. (11).

$$P_k = \mu_t \left( \frac{\partial U_i}{\partial x_j} + \frac{\partial U_j}{\partial x_i} \right) \frac{\partial U_i}{\partial x_j} - \frac{2}{3} \frac{\partial U_k}{\partial x_k} \left( 3\mu_t \frac{\partial U_k}{\partial x_k} + \rho k \right) \quad (11)$$

The terms  $P_{\omega b}$  and  $P_{kb}$ , are defined by Eq.(12).

$$P_{\omega b} = P_{kb} = g_i \frac{\mu_t}{\sigma_{\theta}} \frac{\delta \bar{T}}{\delta x_i} \quad (12)$$

#### 4.2 Discretization:

The discretization of the computational domain was constructed with a non-uniform structured hexahedral mesh in order to increase the amount of elements near the wall, capturing the boundary layer effects ( $y^+ < 1$ ). To achieve such precision, it was used the methodology of [14], where the number of divisions between height ( $h$ ), length ( $b$ ) and fluid channel thickness ( $t$ ) was increased by the ratio of  $\sqrt{2}$  for each numerical simulation.

It was possible to determine that there was a numerical convergence when the dimensionless  $y^+$  was established smaller than the unit for analysis of the natural convection. Other properties were monitored so that the variation of the answer in relation to the previous simulation did not vary more than 0.1%. Among them, the amount of heat transferred, temperature in the location of the thermocouples in the central plate and maximum courant number, which remained lower than the unit during the whole analysis of the natural convection, allowing the correct capture of the thermo-hydraulic effects. Therefore, the final mesh of the fluid domain has 600,000 nodes, with a mean dimension per element of 2.24mm x 1mm x 0.18mm ( $h \times b \times t$ ), with  $h$  height,  $b$  width and  $t$  thickness. Cladding and Meat domain counted 25,000 elements each.

#### 4.3 Boundary Conditions:

To create the initial conditions of the transient analysis, the central fuel plate with nominal IFA flow rate of 6.27 kg/s was simulated. Based on the studies of [15], it is known that the flow distribution between the channels is not homogeneous, however, a 3.2% lower flow rate (0.357 kg/s) was adopted due to the effect of the fuel support pin. The axial power profile is illustrated

in Figure 5 where the dimension at 0 cm is the upper region (nominal inlet) and 600 cm is the lower region (nominal outlet), i.e., closer to the bottom of the pool.

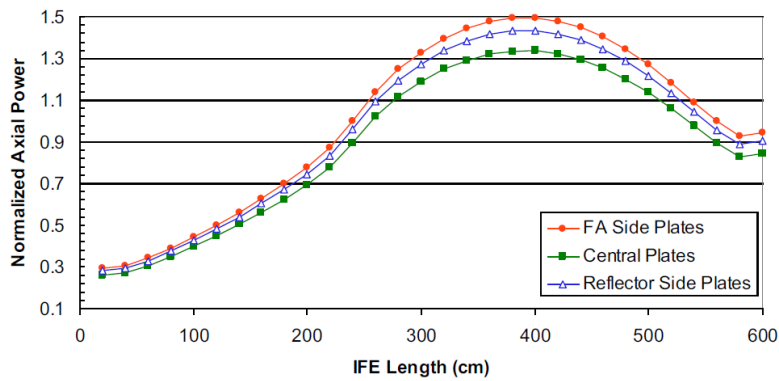


Fig.5 – Axial power density for FA Side, Central and Reflector side plates.

For the transient analysis, the decay power is approximated (with coefficient of determination  $R^2 = 0.9952$ ) by Eq. (13), where  $t$  is the time in seconds after the reactor shutdown (SCRAM) that results in the power percentage in relation to the nominal power immediately before the shutdown, which in this study represents 3.5 MW.

$$\%Pot = -1,077 * LN(t) + 8.8677 \quad (13)$$

The other boundary conditions used in the modeling are described below:

- i. Non-slip condition (fluid velocity equal to zero at surface)
- ii. Constant pool temperature at 32.7°C
- iii. Average hydrostatic pressure: 1.75 bar
- iv. Condition of double axial symmetry, simulating one fourth of the meat, cladding and flow channel.
- v. The fluid used for water analysis and all thermodynamic properties were determined according to the IAPWS recommendation [12], since the density is not kept constant, so the source term of the momentum conservation equation is constantly recalculated along the flow.

#### 4.4 Solver options and convergence criteria:

The advection and diffusion scheme is described in the program as "High Resolution Scheme" [16] [11], preventing the creation of numerical peaks of the properties between the nodes, increasing the computational time, but the analysis becomes more stable when compared with Upwind model.  $10^{-5}$  for the convergence criteria of root mean square.

### 5. Results:

The presented results are necessary to make a comparison between experimental [9].

#### 5.1 Coolant Temperature Difference

As the present work presents a flow inversion, the use of the terms of inlet and outlet of the fuel assembly does not become didactic, since at a given moment the regions change their function. Thus, Figure 6 illustrates a comparison of the experimental and numerical results for the temperature difference between the upper (nominally the inlet) and lower0 regions (nominally the outlet).

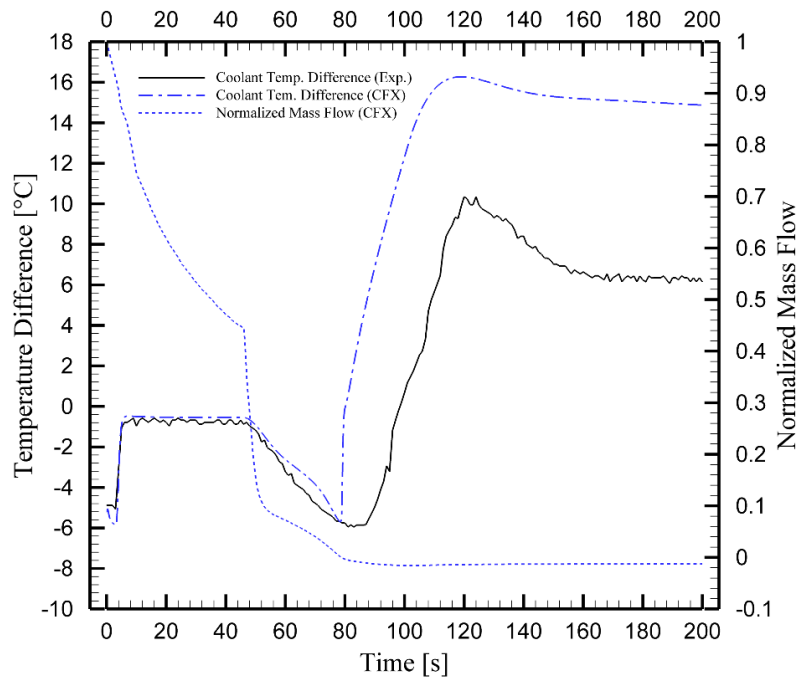


Fig 6. Coolant temperature difference comparison and normalizes mass flow

To explain some observed phenomena, the analysis will be divided into three major steps.

The accident starts when the centrifugal pump is turned off, which after 3 seconds the flow drops to 93% of its initial value; Due to this, the reactor is programmed to shut down (SCRAM). From this moment and until 45s, the flow is reduced gradually due to the inertia flywheel. In this step, the promoted flow is able to remove almost all the heat generated inside the core, causing a very small variation of temperature ( $\sim 0.5^{\circ}\text{C}$ ).

At the second step, the coupling valve is open at 46s due to the small pressure difference, which results in a huge mass flow drop inside the fuel assemblies. The resulting mass flow continues to decrease to zero, initiating the natural convection phenomenon at 87s (Exp.) or 79s (CFX).

The third stage is characterized by the evolution of natural convection. The flow growth until the heat removal capacity and the heat generated are the same: 123s (Exp.) or 119s (CFX). From this moment and beyond, the ability to remove heat is greater than that generated, gradually reducing the temperature difference.

Finally, the data presented a good correlation up to 80 seconds (end of forced convection), initiating some difference between the numerical data and those obtained experimentally. Among the justifications for the difference would be that the pool temperature cannot be considered constant, since when the inversion starts, the upward fluid will be that heated throughout the downward process, not the pool average ( $32.7^{\circ}\text{C}$ ).

## 5.1 Clad Temperatures

The safety criteria of the research reactor states that the cladding temperature should remain below  $90^{\circ}\text{C}$ . Figure 7 presents the comparison of the temperatures collected in the thermocouples: TC3, TC6 and TC10 (Figure 1).

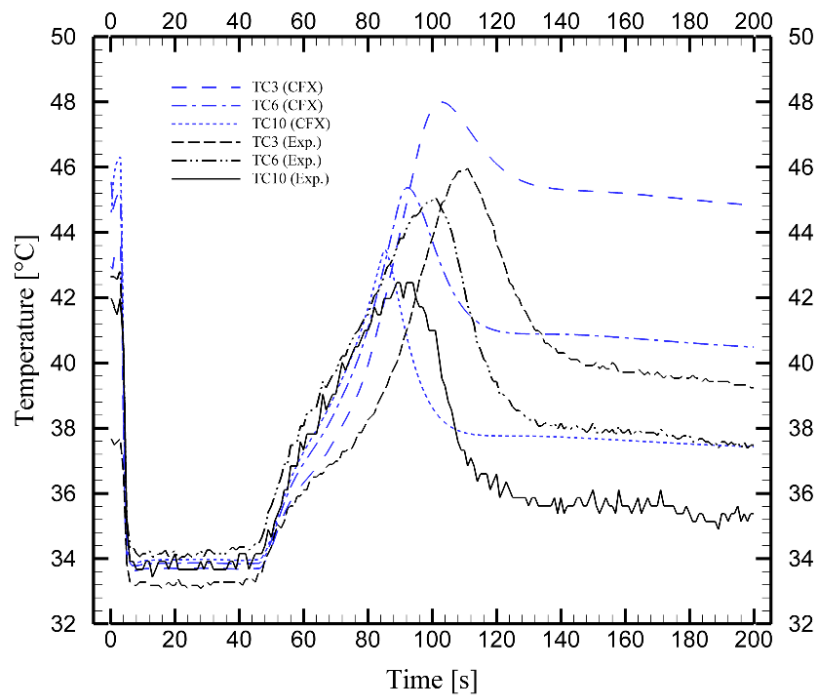


Fig 7. Thermocouple comparison between experimental and numerical data

Initially (0s) there is a large difference between the steady state temperatures (3.5MW); however, the total heat transferred has an error less than 6%. This behavior can be coupled so that the axial power distribution of numerical does not match the experimental profile. The temperature peaks presented conservative results in relation to the experimental ones, since these were up to 4% hotter and 3.7% later. However, analyzing the whole simulation, the numerical response was able to predict the qualitative behavior with a maximum deviation of 16% at the 200s of the TC10 thermocouple.

Although the numerical model did not consider the variation of the pool temperature, the numerical results showed a satisfactory similarity with the experimental data

### Conclusion:

A LOFA transient numerical analysis was performed for the nuclear research reactor IEA-R1 with commercial code ANSYS-CFX<sup>®</sup> [18]. The study is in its initial phase, where the presented model is able to predict all the thermo-hydraulic effects observed experimentally.

The initial results point to great qualitative similarity with the experiments, nevertheless, some adjustments in the numerical model are necessary. The calculated maximum deviation was 16% for the cladding temperature (TC10) at 200s, which should be investigated.

Among the future improvements, the constant pool temperature should be analyzed to better understand its effect and influence, and the axial power distribution in the central plate should be analyzed more rigorously. A more appropriate model is under development and will be published soon.

### Acknowledgments:

The authors would like to acknowledge IPEN, for infrastructure and the International Atomic Energy Agency (IAEA) for the financial assistance to participate in the RRFM 2018.

## References

- [1] D. D'Auria, F., Bousbia-Salah, A., Galassi, G.M., Vedovi, J., Reventós, F., Cuadra, A., Gago, J.L., Sjöberg, A., Yitbarek, M., Sandervag, O., Garis, N., Anher, C., Aragonés, J.M., Verdù, G., Mirò, R., Ginestar, D., Sánchez, A.M., Maggini, F., Hadek, J., Macek, "Neutronics/Thermal-hydraulics Coupling in LWR Technology: State-of-the-art Report (REAC-SOAR)," *Nucl. Energy Agency*, vol. NEA N° 543, 2004.
- [2] IAEA Publications, "Research Reactor Benchmarking Database: Facility Specification and Experimental Data," 2015.
- [3] A. Hainoun and A. Schaffrath, "Simulation of subcooled flow instability for high flux research reactors using the extended code ATHLET," *Nucl. Eng. Des.*, vol. 207, no. 2, pp. 163–180, Jul. 2001.
- [4] A. Hamidouche, T., Bousbia-Salah, "RELAP5/3.2 assessment against low pressure onset of flow instability in parallel heated channels," *Ann. Nucl. Energy*, vol. 33, pp. 510–520, 2006.
- [5] F. Hamidouche, T., Bousbia-Salah, Al Khider, S., D'Auria, "Overview of accident analysis in nuclear research reactors," *Progr. Nucl. Energy*, vol. 50, pp. 7–14, 2008.
- [6] F. Hamidouche, T., Bousbia-Salah, Al Khider, S., Yazid Mokeddem, M., D'Auria, "Application of coupled code technique to a safety analysis of a standard MTR research reactor," *Nucl. Eng. Des.*, vol. 239(10), pp. 2104–2118, 2009.
- [7] A. Omar, H., Ghazi, N., Alhabit, F., Hainoun, "Thermo-hydraulic analysis of Syrian MNSR research reactor using RELAP5/Mod3.2 code," *Ann. Nucl. Energy*, vol. 240(5), pp. 1132–1138, 2010.
- [8] Hainoun, A., Hicken, E., Wolters, J., "ATHLET-extension for application research reactors," *Proc. Annu. Meet. Nucl. Technol.*, 1993.
- [9] A. Hainoun *et al.*, "International benchmark study of advanced thermal hydraulic safety analysis codes against measurements on IEA-R1 research reactor," *Nucl. Eng. Des.*, vol. 280, pp. 233–250, Dec. 2014.
- [10] P. E. Umbehaun, "Description of IEA-R1 Research Reactor," *Inst. Pesqui. Energéticas e Nucl. (IPEN / CNEN - SP)*, 2012.
- [11] Ansys Inc., "Ansys CFX - Solver Theory Guide." 2006.
- [12] H. J. Wagner, W. ; Kretzschmar, "IAPWS industrial formulation 1997 for the thermodynamic properties of water and steam," *Int. Steam Tables Prop. Water Steam Based Ind. Formul. IAPWS-IF97*, p. 7–150., 2008.
- [13] D. C. Wilcox, *Turbulence modeling for CFD*, 1st ed. California: Glendale: DCW Industries., 1993.
- [14] E. G. Stern, F.; Wilson, R. V.; Coleman, H. W.; Paterson, "Comprehensive approach to verification and validation of CFD simulations-Part 1: methodology and procedures," *Trans. Soc. Mech. Eng. J. Fluids Eng.*, vol. 123(4), pp. 793–802, 2001.
- [15] J. A. B. Torres, W.M., Umbehaun, P.E., Andrade, D.A., Souza, "A MTR fuel element flow distribution measurement, preliminary results," *Int. Meet. Reduc. Enrich. Res. Test React.*, vol. Chicago, I, no. October, pp. 5–10, 2003.
- [16] J.-L. Yee, H. C., Klopfer, G. H. & Montagne, "High-resolution shock-capturing schemes for inviscid and viscous hypersonic flows," *J. Comput. Phys.*, vol. 88(1), pp. 31–61, 1990.